Electronic Supplementary Material (ESI) for Journal of Materials Chemistry A.

Supporting Information

Photo-switchable membranes constructed from graphene oxide/star-PDMS nanocomposites for gas permeation control

Abdalrahman U. Alrayyes, Yaoxin Hu, Rico F. Tabor, Huanting Wang and Kei Saito*

Abstract: A novel photo-responsive membrane based on a star-shaped polydimethylsiloxane (PDMS) polymer and graphene-based nanosheets was for the first time designed and fabricated for controlling gas permeation. The sub-60 nm thick membrane exhibited continuous photo-reversible gas permeance control when irradiated with UV light of variable wavelengths. By optimising the nanosheet loading and nanosheet-polymer interface, the defect-free membrane demonstrated satisfactory gas separation performance towards CO_2 and C_3H_8, allowing the membrane to be potentially be useful as a photoresponsive coating for applications such in modern plant cultivation technologies.The effect of the nanosheets on the photo-triggering mechanism, a [2+2] cycloaddition reaction was investigated, which revealed that the presence of the nanosheets improved the polymerization reaction, but hindered the de-polymerisation reaction. This work provides a new opportunity for the production and investigation of a new class of photo-responsive two-dimensional nanocomposite membranes for highly controlled molecular/ion sieving.

SUPPORTING INFORMATION

Table of Contents

Item	Pages
Experimental methods	3-4
Characterisation methods	4
Scheme S1. Synthesis of polymers	5
Figure S1. FT-IR spectra of APTS-GO before and after UV irradiation	6
Figure S2.XRD spectra of APTS-GO, GO	6
Figure S3. XPS spectra of APTS-GO, GO	7
Figure S4. ^{1}H NMR of sPDMS-32 step 1	8
Figure S5. ^{1}H NMR of sPDMS-32 step 3	8
Table S1. M_w of polymers from GPC and NMR	9
Figure S6. SEM images of the composite membranes	9
Figure S7. SEM images marked with graphene	10
Figure S8. SEM image showing the wrinkled graphene surface	10
Figure S9. AFM of the composite membranes	11
Table S2. Single gas permeances of the composite membranes	12
Table S3. Ideal selectivities of the composite membranes	12
Figure S10. UV-gas permeance response for the composites (0.1, 0.25, 0.75)	12
Figure S11. XRD spectra of sPDMS, composite, and composite after UV exposure	13
Figure S12. DSC curves of the composites	14
Figure S13. Zoomed out DSC curve	15
Figure S14. TGA curves of the composites	15
Figure S15. UV-Vis spectra of sPDMS, and the composite APTS-GO/sPDMS	16
Table S4. UV reaction kinetics analysis from UV-Vis	16
Table S5. Statistics of permeability, solubility and diffusion of gases in PDMS	17
Figure S16. Optical images of precursor solution and membrane	17
References	17

SUPPORTING INFORMATION

Experimental Procedures

Materials

All chemicals purchased were used without further purification. The following chemicals were purchased from Sigma Aldrich (NSW, Australia: Platinum(0)-1,3-divinyl-1,1,3,3-tetramethyldisiloxane complex solution (Karstedt's catalyst), 7-hydroxycoumarin, allyl bromide, potassium carbonate, anhydrous magnesium sulfate, (3-Aminopropyl)triethoxysilane (APTS), and N,N'-Dicyclohexylcarbodiimide (DCC). p-Toluenesulfonic acid (triflic acid) (99%+) was purchased from Ajax Chemicals (NSW, Australia). Tetrakis(trimethylsilyloxy)silane (TDMSS) and hexamethylcyclotrisiloxane (D3) were purchased from Gelest, Inc. (PA, USA). Whatman™ anodised aluminium oxide porous discs (Anodisc®), AAO, with a 13 mm diameter and 100 nm pores were obtained from bio-strategy (VIC, Australia) and were used as membrane substrates. Graphene oxide dispersions in water (1mg/ml) with a sheet size >500 nm were purchased from XFNano (Nanjing, China) Item code: XF020.

Synthesis of the star-shaped polymer, sPDMS-H, following a similar method in literature:[1]

Step 1: polymerisation of TDMSS to form siloxane core terminated with hydrosilane 'sPDMS-X-H' where X is number of repeating -Si(CH$_3$)$_2$-O- units per arm

For sPDMS-24-H: In a round-bottom flask and under N_2 flow, TDMSS (0.17 mmol, 0.06 g) and D3 (5.52 mmol, 1.23 g) (1:32 molar ratio TDMSS:D3) were dissolved in anhydrous methylene chloride (3 ml) at 25 ^oC. After dissolution of the reactants, triflic acid (3 µl) was added and the reaction was magnetically stirred for 5 minutes. Anhydrous potassium carbonate (105 mg) and 20 ml of methylene chloride were then added to quench the reaction. The mixture was filtered and washed with 20 ml of DI water. The volatile fraction was separated and dried over anhydrous magnesium sulfate, and filtered. Finally, the solution was dried under reduced pressure to obtain sPDMS-24-H as a colourless oil (1.10 g, 86% yield by mass). ^{1}H-NMR δH (400 MHz; (CD$_3$)$_2$SO): 0.01-0.03 (m, -Si(C$\mathbf{H_3}$)$_2$-O-), 0.04-0.06 (m, -Si(C$\mathbf{H_3}$)$_2$-H), 4.62 (m, -Si(CH$_3$)$_2$-**H**.

sPDMS-3-H: The same procedure was carried out as above, but with changing in the TDMSS: D3 molar ratio to 1:4, where TDMSS (2.17 mmol, 0.51 g) and D3 (8.67 mmol, 1.92 g) were used. The obtained product was a colourless oil (1.76 g, 73% yield by mass).

Step 2: Synthesis of 7-(allyloxy)-coumarin
Into a round-bottom flask, 7-hydroxycoumarin (26.30 mmol, 4.26 g) was dissolved in 65 ml of acetone, followed by addition of potassium carbonate (78.65 mmol, 10.87 g) and allyl bromide (76.95 mmol, 9.31 g). The continuously stirred mixture was then heated to 70 ^oC for 14h. After cooling to room temperature, the mixture was filtered and dried under reduced pressure to obtain the off-white powder product (3.35 g, 63% molar yield). ^{1}H-NMR δH (400 MHz; CDCl$_3$): 4.68 (d, CH$_2$=CHC$\mathbf{H_2}$O–, 2H), 5.31-5.46 (d, , C$\mathbf{H_2}$=CHCH$_2$O–, 2H), 6.05 (m, CH$_2$=C**H**CH$_2$O–, 1H), 6.25 (d, ArH, 1H), 6.82 (d, ArH, 1H), 6.86 (d, ArH, 1H), 7.37 (d, ArH, 1H), 7.63 (d, ArH, 1H).

Step 3: Attachment of Step 2 product to Step 1 product via hydrosilylation to obtain coumarin-terminated sPDMS
sPDMS-24: Into a round-bottom flask, step 1 product, sPDMS-24-H (0.08 mmol, 0.59 g), and step 2 product (0.79 mmol, 0.16 g) were dissolved in toluene (3 ml). Next, Karstedt's catalyst (7 µl) was added and the continuously stirred mixture was heated to 70 ^oC for 3.5 h. After cooling to room temperature, the mixture was added dropwise to hexane (30 ml) while swirling the hexane flask by hand. The hexane/toluene solution was purified by successive washes with N,N-Dimethylformamide (15 ml) and then methanol (15 ml). Finally, the hexane/toluene layer was dried under reduced pressure to obtain the final, slightly yellow viscous oil (0.47 g, 71% yield by mass). ^{1}H-NMR δH (400 MHz; CDCl$_3$): 0.007-0.26 (m, -Si(C$\mathbf{H_3}$)$_2$-O-), 0.65 (m, –Si(CH$_3$)$_2$C$\mathbf{H_2}$CH$_2$CH$_2$O–, 8H, or 2 per arm), 1.85 (m, –Si(CH$_3$)$_2$CH$_2$C$\mathbf{H_2}$CH$_2$O–, 8H, or 2 per arm), 3.98 (m, –Si(CH$_3$)$_2$CH$_2$CH$_2$C$\mathbf{H_2}$O–, 8H, or 2 per arm), 6.24 (d, ArH, 4H, or 1 per arm), 6.81 (d, ArH, 4H), 6.84 (d, ArH, 4H, or 1 per arm), 7.34 (d, ArH, 4H, or 1 per arm), 7.63 (d, ArH, 4H, or 1 per arm).). IR (cm^{-1}): 864, 787, 1009, 1076, 1258, 1404, 1509, 1616, 1750, 2963.

sPDMS-3: The same procedure was carried out as above, but using sPDMS-3-H (0.77 mmol, 0.94 g) with step 2 product (7.95 mmol, 1.61 g) with the same amounts of toluene and catalyst. The obtained product was a slightly yellow viscous oil (0.30 g, 20% yield by mass).

Synthesis of aminosilane-functionalized graphene oxide (APTS-GO)

Functionalization of GO with APTS was done using a commonly reported technique, whereby APTS reacts with the hydroxyl, epoxide, carboxyl and carbonyl groups on the GO's surface using DCC as the catalyst.[2, 3]

25 ml of the as-received graphene oxide (GO) dispersion in water (1mg/ml) was placed in a falcon tube, frozen in liquid N_2, and freeze-dried for 1 week. The tube was washed with 25 ml of APTS and the contents were poured into a round-bottom flask to ensure no loss of GO powder. 12.5 mg of DCC was added to the flask, and the mixture was tip-sonicated (BRANSON Sonifier® SFX550 550W max. power, 20kHz**,** 10% amplitude, 1 second on, 2 seconds off) for 1 hour (total on time) in an ice bath maintained below 10 ^oC. A magnetic stirring bar was inserted, and the mixture was stirred and reacted at 70 ^oC for 24h. After cooling to room temperature, the mixture was centrifuged (9000 rpm, 30 min.). The supernatant was poured out, and the nanosheet sediment was washed three times with a 1:1 DI water: tetrahydrofuran (THF) mixture, with water bath

sonication for 5 min. and centrifugation at 9000 rpm for 20 min. done in between washes, hence neutralising the solution to pH 7. The washing, sonication, and centrifugation steps were repeated 4 additional times with pure THF to remove the water. Finally, the nanosheets were made into a 1 mg/ml THF suspension by water-bath sonication for 2 hours (<20 ^{o}C) and stirring overnight.

Nanocomposite membrane fabrication

Precursor solution

Prior to use, the APTS-GO suspension was water bath sonicated for 1 hour (<20 ^{o}C). The precursor solution contained either sPDMS-24 or sPDMS-3 and APTS-GO in THF. The weight of the polymer was set to 4% in THF, and the weight ratio of the polymer/APTS-GO was varied from 0.1 to 0.75%. The chosen total wt.% solution concentration played a key role in the membrane formation, as the liquid polymer could not form an adequately viscous precursor solution, meaning that at a lower wt.%, not enough polymer stayed on the substrate, forming a defective membrane. In a typical procedure (4% in THF, 0.5% APTS-GO/sPDMS-24), sPDMS-24 (17.6 mg) was dissolved in THF (412 µl). The 1mg/ml APTS-GO in THF dispersion (88 µl) was added dropwise to the polymer solution under vigorous magnetic stirring. The solution was stirred for 1 hour, water bath sonicated for 1 hour (40 ^{o}C), and subjected to multiple short cycles of vacuum to remove air bubbles.

Fabrication

The AAO substrate was taped onto a glass slide, which was placed on a spin coater. 70 µl of the precursor solution was dropped on the substrate for 2 seconds, and then the spinning was initiated (700 rpm/s, 1500 rpm, 30 s). The membrane was dried under vacuum at 65 ^{o}C for 30 min., and subsequently subjected to 365 nm irradiation for 10 min. The coating/drying/UV irradiation steps were repeated 2 additional times, but with dropping 150 µl of the precursor solution onto the substrate after reaching full speed.

Characterisation

SEM images were captured using a FEI Nova NanoSEM 450 FEGSEM at an accelerating voltage of 5 kV. Samples were carbon-taped to a stud and coated with iridium. UV-Vis measurements were obtained using a UV-1800 Shimadzu spectrophotometer using quartz slides as sample supports. FT-IR spectra were obtained using an Agilent Cary 630 FTIR spectrometer, using 32 scans at a resolution of 4 cm^{-1}. UV-irradiation was performed using a CL1000M UV-cross-linker lamp (UVP LLC., Australia) which provided polychromatic light centred at 365 nm and 254 nm in an open-air environment. ^{1}H NMR spectra were obtained using a Bruker DRX 400 instrument. DSC measurements were obtained using a PerkinElmer DSC-8000 which utilized a nitrogen purge. TGA curves were obtained using a Mettler TGA/DSC1 star system.

Results and Discussion

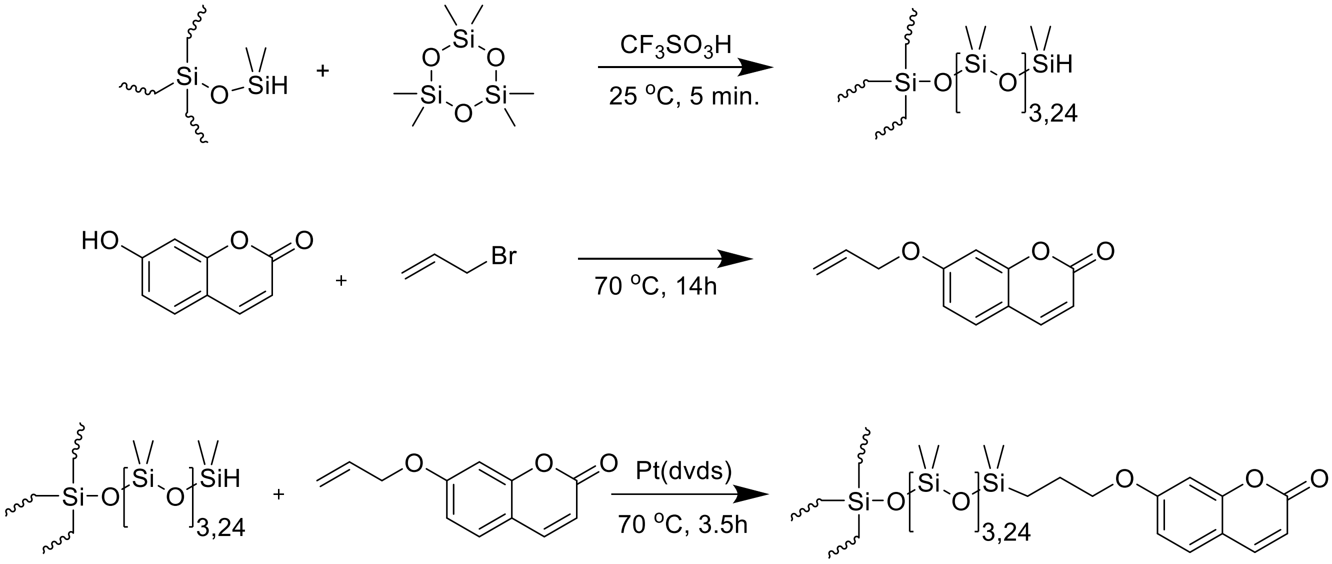

Scheme S1. Reaction pathway towards the synthesis of sPDMS-24 or sPDMS-3. The curled lines represent arms identical to the arm illustrated in the scheme.

The star-shaped polymer was synthesised following a two-step procedure previously reported by Honda and Toyota.[1] The first step involved a cationic ring-opening polymerization reaction between tetrakis(dimethylsiloxy)silane (TDMSS) and hexamethylcyclotrisiloxane (D3) to form a 4-arm structure terminated with silane units. The length of the chains on each arm was controlled by varying the ratio between D3 and TDMSS. In this study, 3 and 24 -$Si(CH_3)_2$-O- repeating units per arm were chosen for a comparative membrane performance study. The 24 repeating unit polymer was chosen based on optimization of the membrane fabrication process, which was tuned by balancing the spin-coating solution concentration, the gas selectivity, and the adhesion between polymer and nanofiller. The second step involved a hydrosilylation reaction between the terminal silane units of step 1 product and 7-(allyloxy)coumarin, finally forming the star-shaped polydimethylsiloxane terminated with coumarin moieties (sPDMS), as depicted in Scheme S1.

SUPPORTING INFORMATION

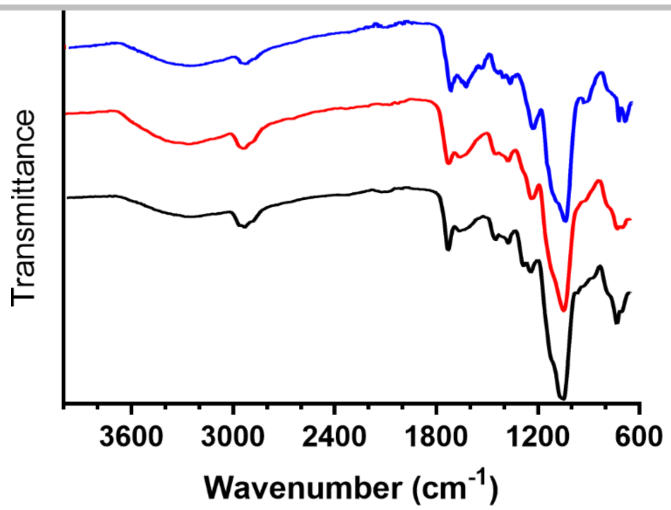

Figure S1. FT-IR spectra of APTS-GO pre-UV (black), after 365 nm irradiation (red), and after 254 nm irradiation (blue). Samples were prepared by drop casting the APTS-GO dispersion on a glass slide, testing FT-IR, irradiating the sample and re-testing FT-IR. The spectra demonstrate that APTS-GO is unaffected by UV irradiation due to the persistence of peaks and unshifting wavenumbers at 3393, 2955, 1721, 1421, 1041, 969 and 727 cm^{-1}, as described in the main text.

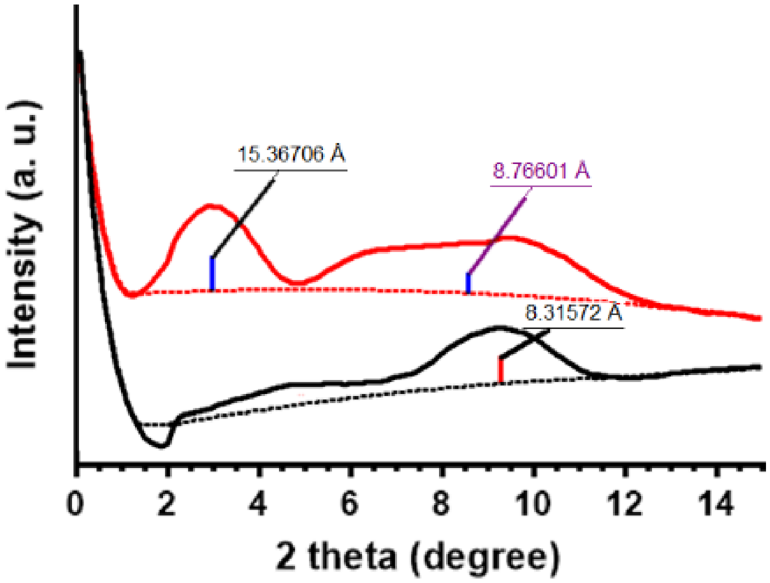

Figure S2. XRD spectra of GO (black) and APTS-GO (red). Samples were prepared by vacuum filtration of the dispersions through a porous nylon filter (200 nm pores) to produce films.

It was clear that GO exhibited a sharp characteristic peak at 2 theta = 10.6°, corresponding to a d-spacing of 8.3 Å. Meanwhile, APTS-GO exhibited a diffraction peak 2 theta = 5.7°, corresponding to a d-spacing of 15.4 Å. The diffraction peak shift was expected since the presence of organosilane functional groups led to a decrease in interlayer stacking, and also proved the successful grafting of APTS on GO. The APTS-GO XRD spectrum also showed a weak diffraction peak at 10.7°, which could have been caused by hydrolysis and subsequent stacking of the sheets during the washing and centrifugation steps.[4]

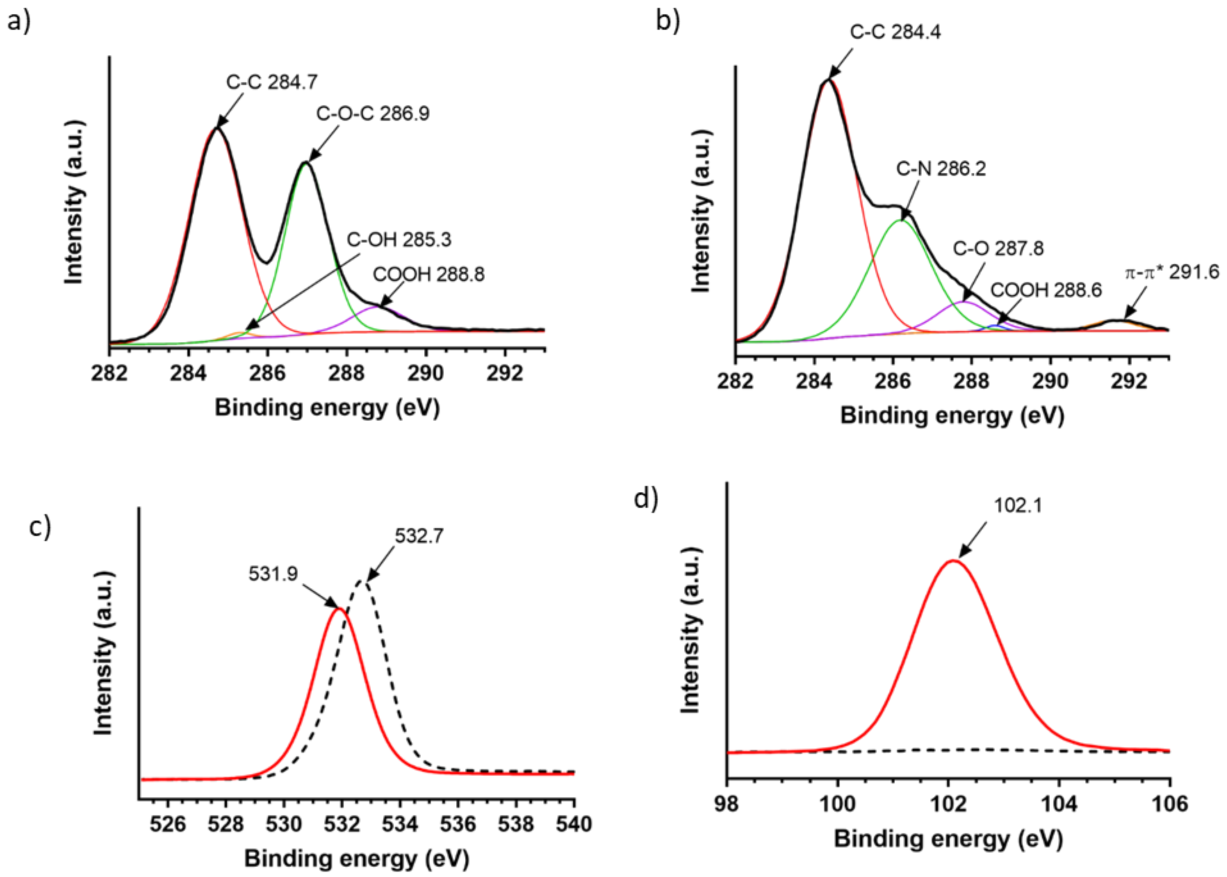

Figure S3. XPS spectra of the nanosheets. a) High resolution C1s spectrum of GO, indicating a high degree of oxidation. b) High resolution C1s spectrum of APTS-GO. c) High resolution O1s spectra of APTS-GO (solid) and GO (dotted). d) High resolution Si2p spectra of APTS-GO (solid) and GO (dotted).

XPS samples were formed by vacuum filtration of GO or APTS-GO dispersions onto porous nylon supports. It was clear that GO underwent a major change in its C1s spectrum post-functionalisation, where the intensity of the C-O peak attributed to epoxy and the COOH peak were dramatically reduced when compared to pristine GO (Figure S3(a)). Furthermore, there was an appearance of a new peak at 286.2 eV attributed to the C-N bond not seen in pristine GO, which proved the successful reaction with APTS's amine and the epoxy groups on GO's surface. Figure S3b shows the O1s spectra of APTS-GO and GO. The O1s peak of GO at 532.7 eV assigned to C-O-C and C=O shifted after functionalization to 531.9 eV in APTS-GO. The shift could be attributed to the newly formed Si-O-Si (or Si-O-C). Altogether, the XPS results strongly confirmed the successful GO functionalization process, which were in-line with the FT-IR results and literature data.[2, 4-6]

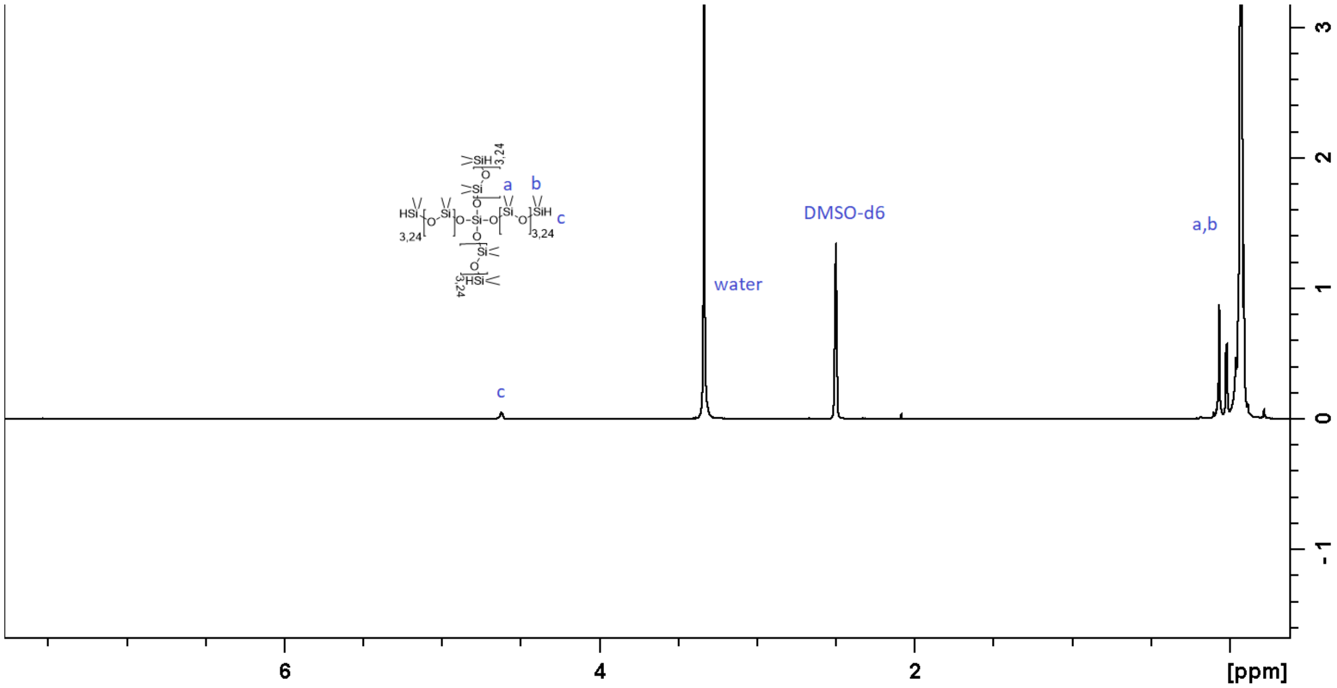

Figure S4. ^{1}H NMR of the step 1 product after the cationic ring opening polymerization between TDMSS and D3. The spectrum is identical regardless of the number of repeating units, except for the amount of Si-CH$_3$ in relation to Si-H.

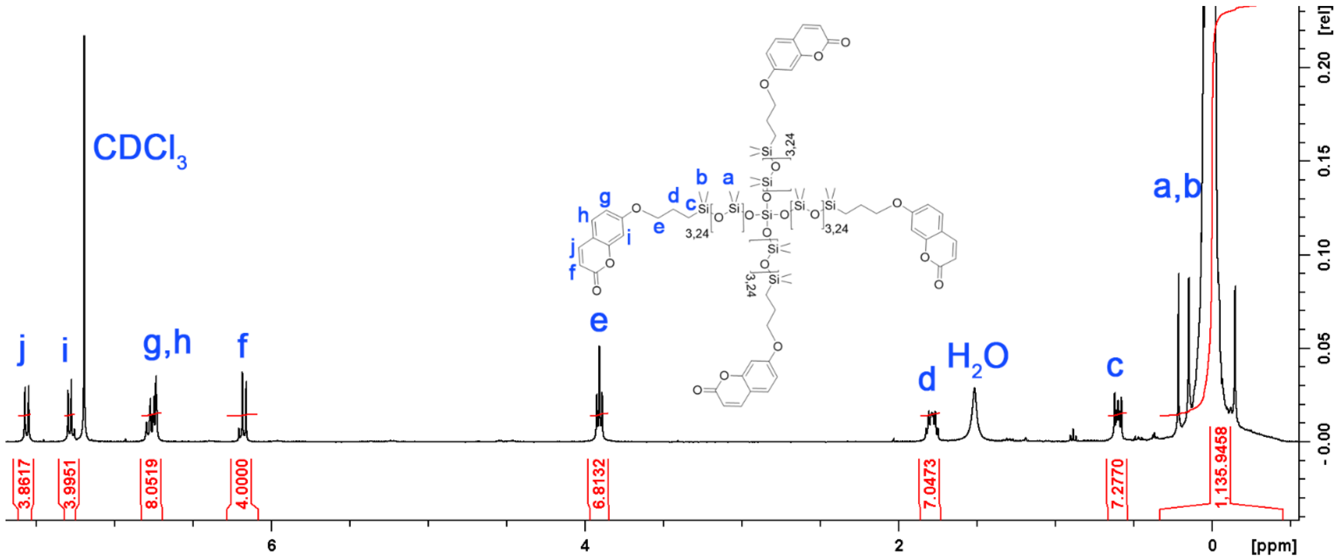

Figure S5. ^{1}H NMR spectrum of the final polymer, sPDMS-24. Theoretical values for c,d,e, are 8, and f,g,h,i,j are 4.

Table S1. Summary of the observed M_n values of both polymers from GPC and ^{1}H NMR compared to the theoretical values.

Polymer	GPC M_n (g mol^{-1}) [a]	GPC M_w/M_n	^{1}H NMR M_n (g mol^{-1}) [b]	Theoretical M_n (g mol^{-1})
sPDMS-3	2380	1.9	2280	2320
sPDMS-24	6810	1.5	14600	8260

[a] Value obtained from RI detector peak using THF as the eluent. The GPC was calibrated with respect to linear polystyrene, which would give inaccurate results for star-shaped polymers, such as the ones used in this study. [b] M_n calculated from the integration value of the Si(**CH_3**) with respect to coumarin.

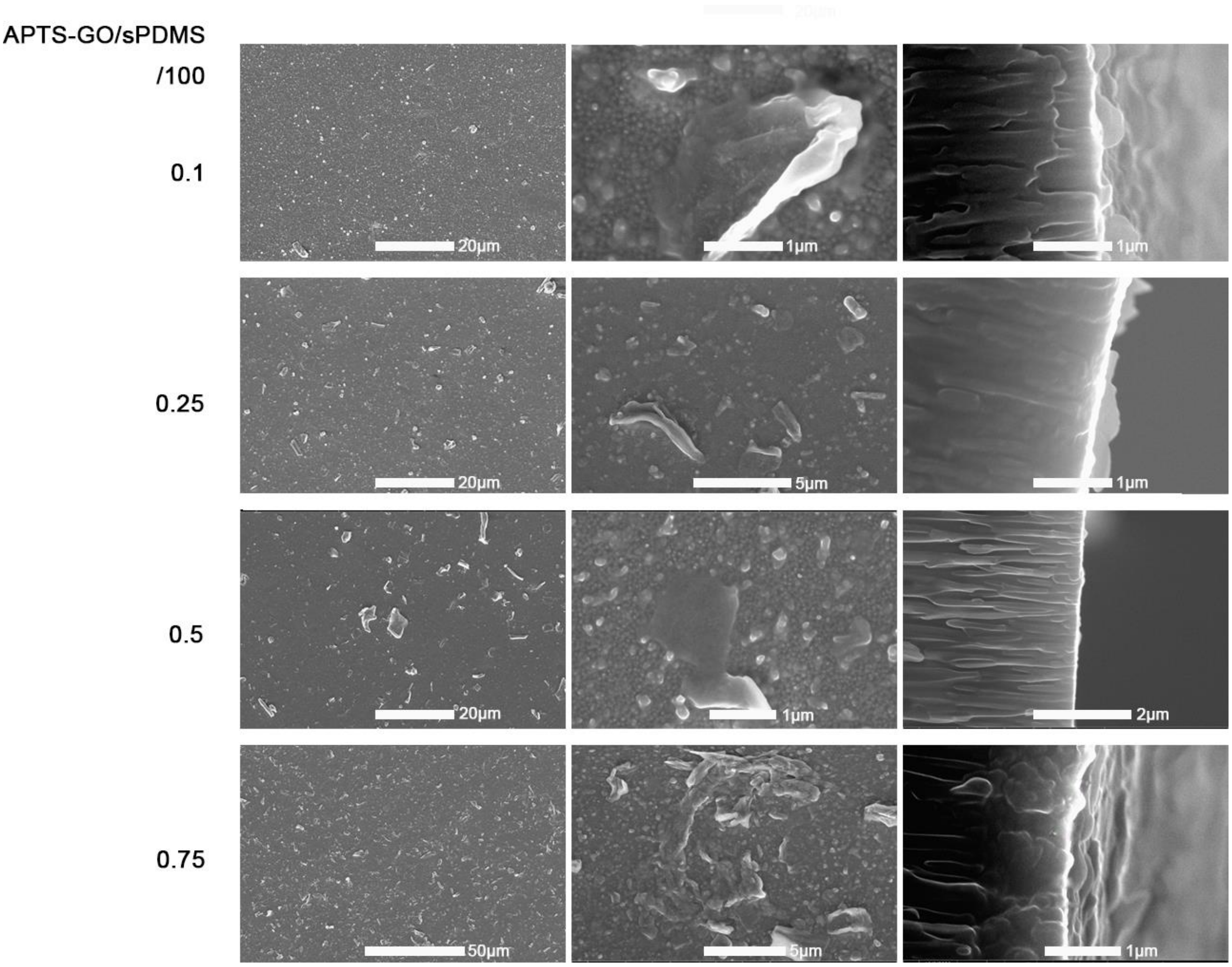

Figure S6. SEM images of various amounts of APTS-GO loadings into the sPDMS membrane. First two columns are topological images, while the last column is cross-sectional images of the membranes. The imaged membranes are the same ones used for the gas permeance study.

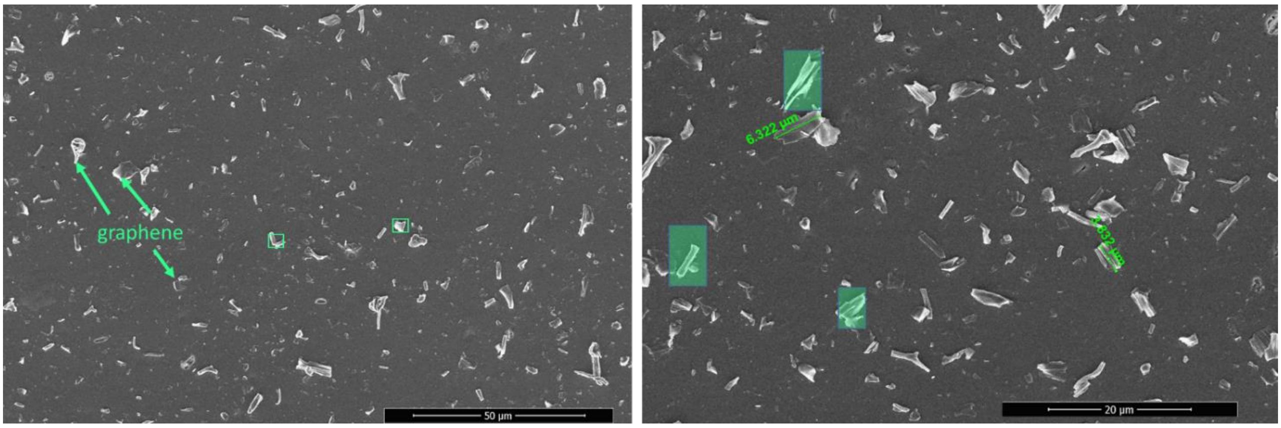

Figure S7. More SEM images indicating the graphene nanosheets. Coloured in areas are the sheets, which contrast with the polymer (dark) due to differences in chemical backbones.

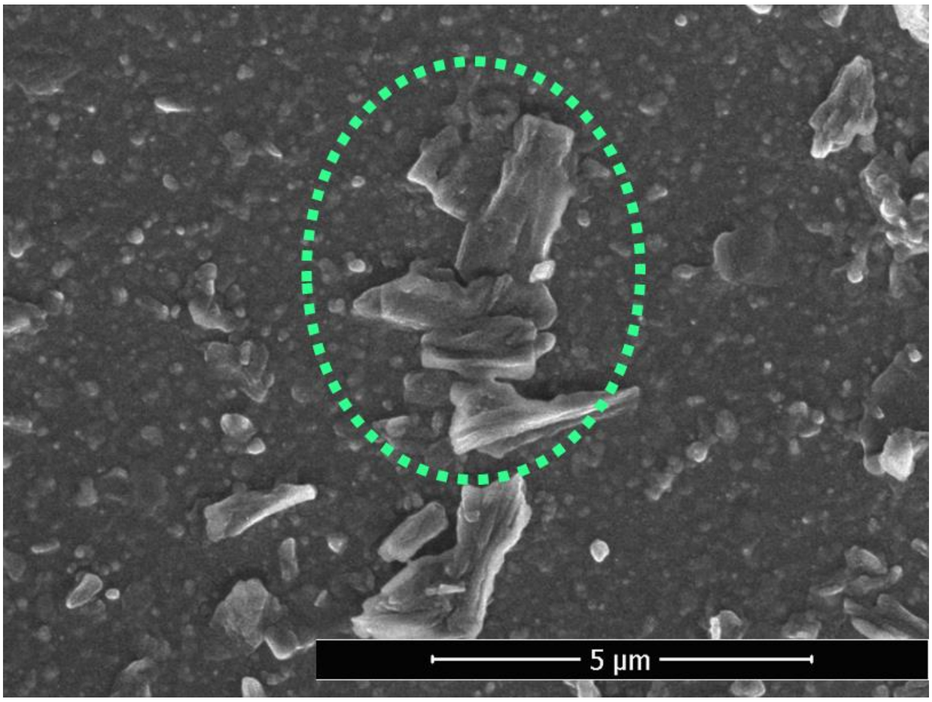

Figure S8. SEM image showing the wrinkled surface of the APTS-GO nanosheets.

For the membrane study, all precursor solutions used a constant 4 wt.% of polymer in THF, and membranes were formed by spin-coating the sPDMS/APTS-GO solutions onto AAO at a constant rate of 1500 rpm. The coating step was repeated a total of 3 times to ensure the complete coverage of AAO, with partial crosslinking *via* 10 min of 365 nm irradiation having been applied between coatings to form layers that would not dissolve by subsequent coatings.

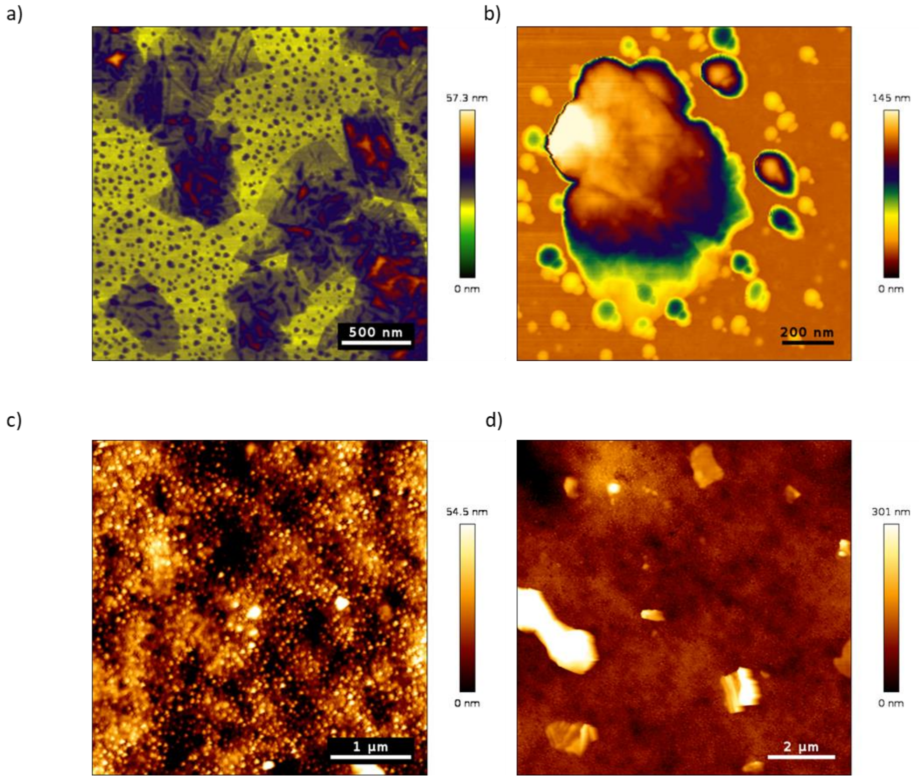

Figure S9. Topological AFM images of a) GO, b) APTS-GO, c) and d) one of the membranes with a 0.5/100 loading of APTS-GO/sPDMS spin-coated onto AAO.

All samples were prepared by spin-coating precursor solutions onto a glass slide. In Figure S8a, it was clear that GO underwent severe wrinkling, which is mainly attributed to the oxygen containing functional groups on its surface, such as the epoxide, which caused wrinkling by interrupting the sp^2 electron network in the bonded carbons.[7] The same phenomenon was observed for APTS-GO in Figure S8b, where the nanosheets underwent an even more pronounced wrinkling effect, possibly due to a greater sp^2 electron interruption by the functionalization process, as observed by a greater z-plane depth range. In both cases, it was evident that the sheets formed 3D structures, as reported previously by Xu *et al.*[8] Another factor supporting the wrinkling argument is the decrease in the AFM apparent lateral sheet size of GO after functionalization.

Table S2. Summary of the single gas permeance values for composites with different APTS-GO loading, as summarised in the main text Figure 3a.

	Single gas permeance (x10^{-10} mol m^{-2} s^{-1} Pa^{-1})				
APTS-GO/sPDMS (x0.01)	N_2	H_2	CO_2	O_2	C_3H_8
0.1	147	478	650	193	961
0.25	58	183	311	81	639
0.5	50	152	354	88	562
0.75	121	368	470	199	780

Table S3. Summary of the ideal selectivity values for composites with different APTS-GO loading, as summarised in the main text Figure 3b.

	Ideal selectivity				
APTS-GO/sPDMS (x0.01)	H_2/N_2	CO_2/N_2	CO_2 / H_2	C_3H_8 /N_2	CO_2/O_2
0.1	3.3	4.4	1.4	6.0	3.4
0.25	3.2	5.4	1.7	5.0	3.8
0.5	3.0	7.1	2.4	11.3	4.0
0.75	3.0	3.9	1.3	6.4	2.3

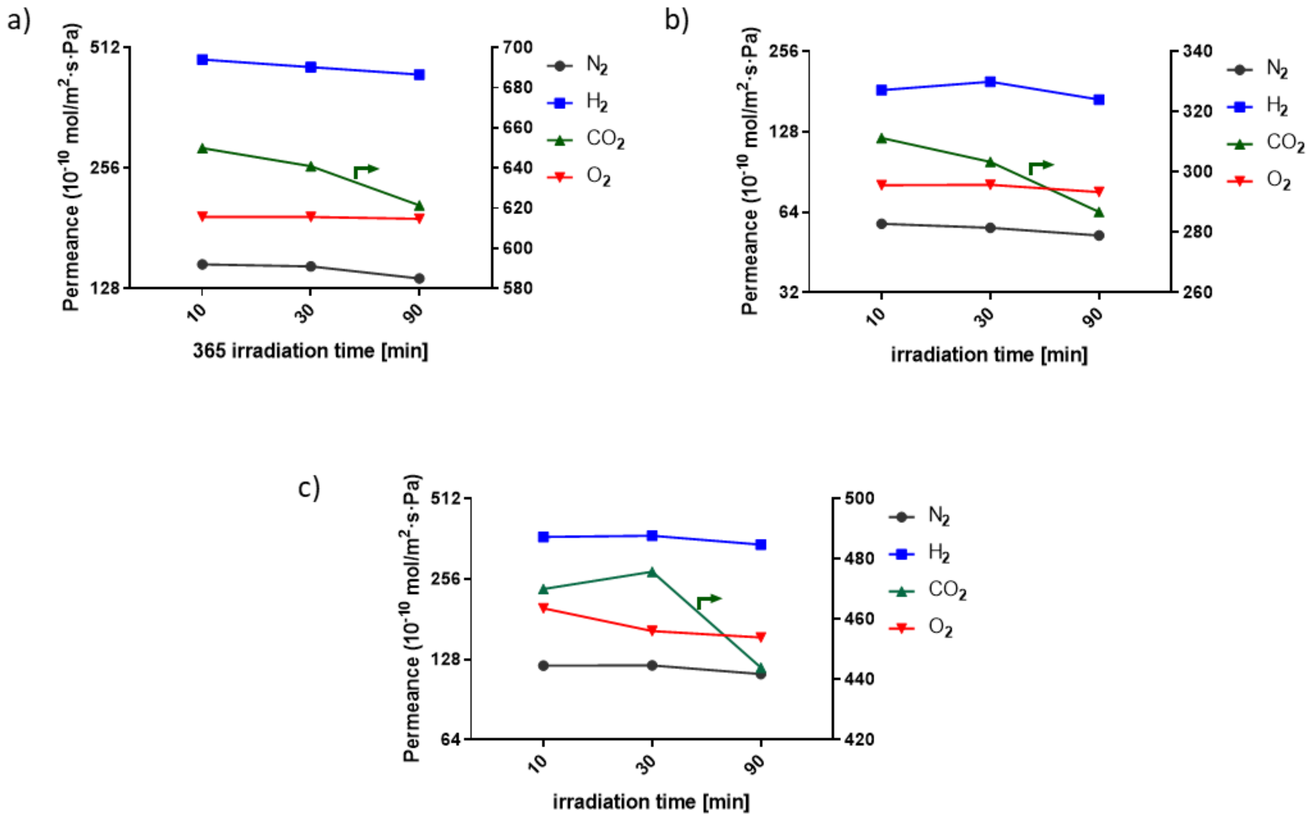

Figure S10. Summary of the permeance response to 365 nm irradiation for membranes containing different loadings of APTS-GO: a) 0.1/100 APTS-GO/sPDMS, b) 0.25/100 APTS-GO/sPDMS, c) 0.75/100 APTS-GO/sPDMS. Testing of the UV response was done by measuring the gas permeances, then irradiating the samples with UV, and then re-testing the gas permeances.

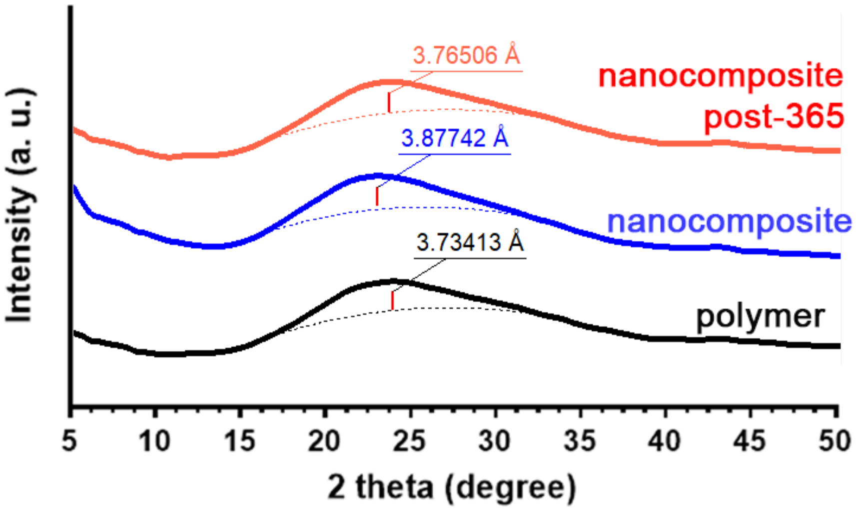

Figure S11. XRD spectra of sPDMS-24 (polymer), 0.5/100 APTS-GO/sPDMS (nanocomposite), and the nanocomposite after 120 min 365 nm irradiation. All samples were made by spin coating a 4 wt.% solution in THF on a glass slide. The shift in d-spacing from polymer to nanocomposite was expected due to the interruption of the polymer matrix by the nanofiller. The shift back to 3.8 Å after crosslinking can be attributed to the increase in polymer chain density due to inter-chain crosslinking.

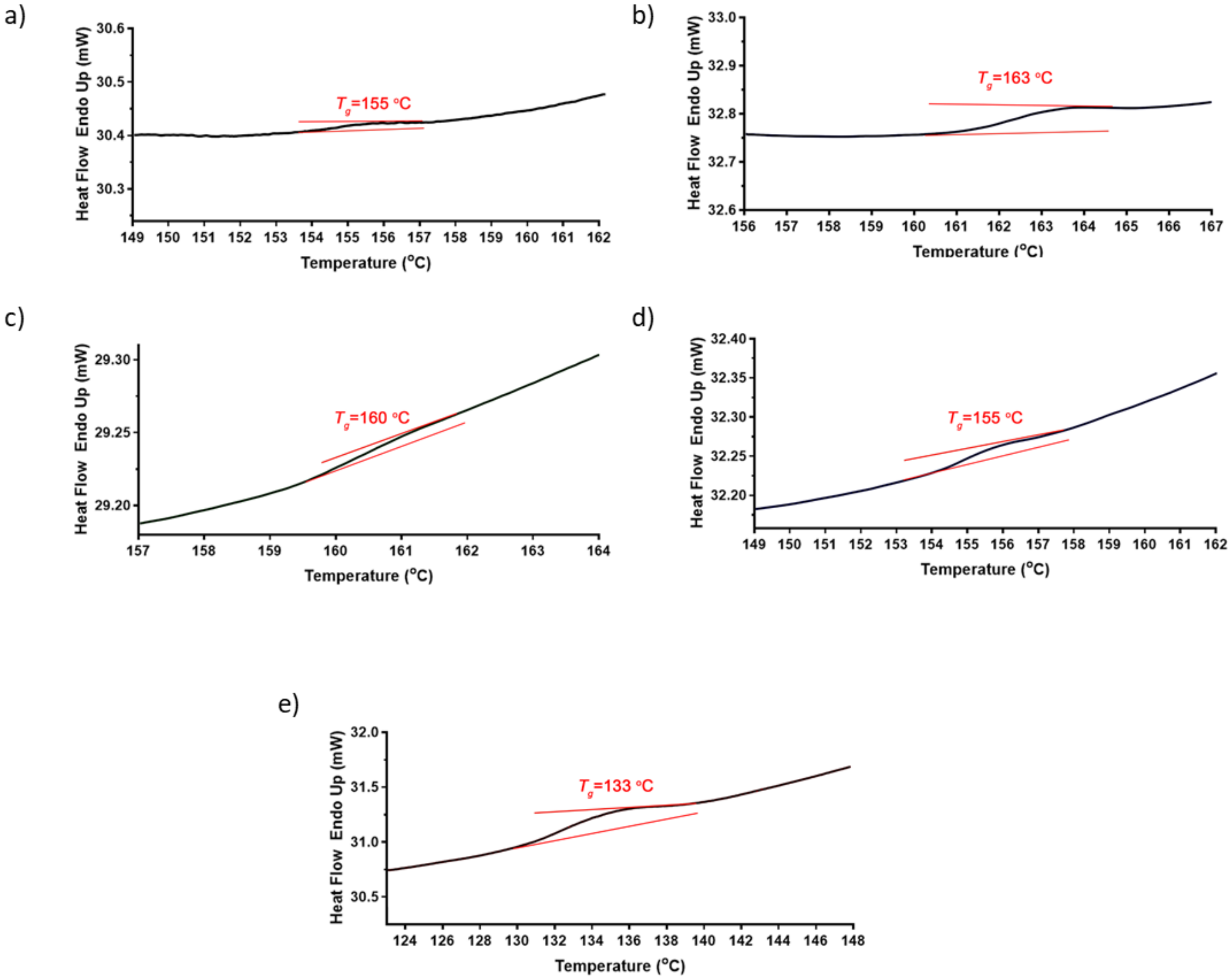

Figure S12. DSC endothermic thermograms for fully crosslinked a) sPDMS-24, b) 0.1/100 APTS-GO/sPDMS composite, c) 0.25/100 APTS-GO/sPDMS composite, d) 0.5/100 APTS-GO/sPDMS composite, e) 0.75/100 APTS-GO/sPDMS composite. All thermograms were obtained using a 50 ^{o}C min^{-1} heating rate, and sample weights were 4-5mg. A typical DSC program was as follows: 1- A temperature scan of 0-200 ^{o}C at 10 ^{o}C min^{-1} heating rate. 2- Isothermal step holding the temperature at 200 ^{o}C for 1 min. 3- A temperature scan of 200-0 ^{o}C at 100 ^{o}C min^{-1} cooling rate. 4- Isothermal step holding the temperature at 0 ^{o}C for 1 min. Steps 1-4 were successively repeated with increasing heat rates of 30, 50, and 80 ^{o}C min^{-1}. Samples were prepared by mixing and sonicating the dissolved polymer (12 wt.% in THF) and the APTS-GO dispersion, followed by casting on a glass slide using a casting knife. The films were then dried and irradiated with 365 nm for 50h to ensure complete crosslinking. Finally, the films were scratched off the slides and placed in the aluminum DSC sample pans.

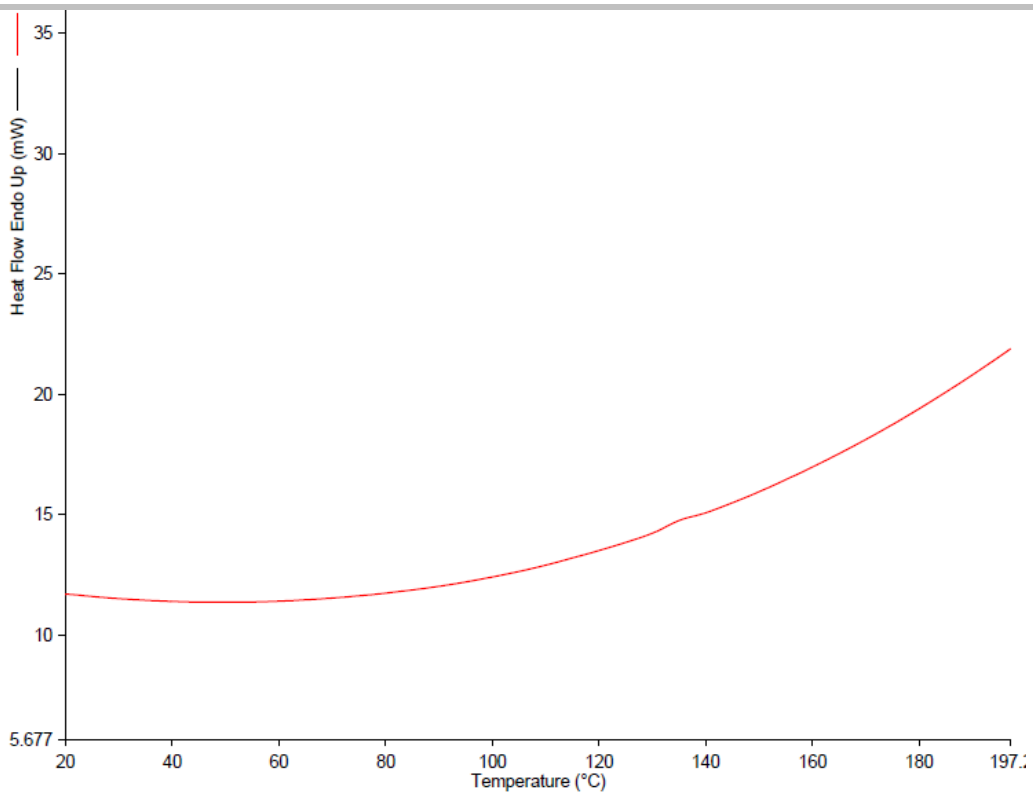

Figure S13. A typical zoomed out DSC endothermic thermogram clearly indicating the T_g of the polymer at around 140 (0.75 wt.% loading).

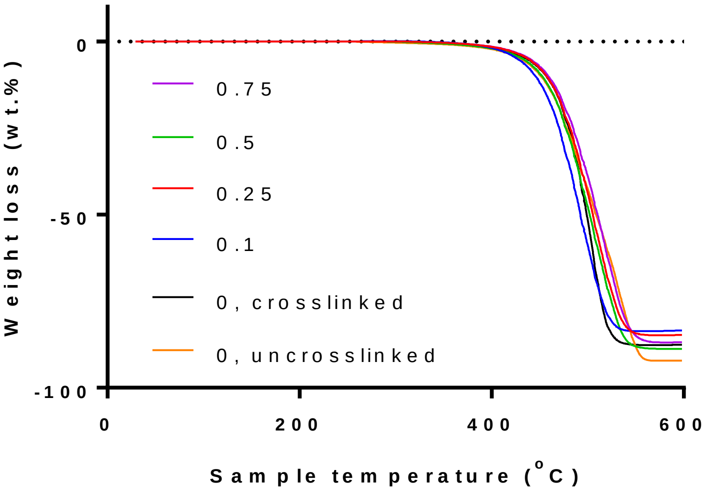

Figure S14. Thermogravimetric analysis (TGA) of the composites and sPDMS-24 alone, with the polymer being analysed before and after crosslinking. The numbers in the legend indicate the ratio of APTS-GO.sPDMS (x0.01), with 0 being the pure polymer. Decomposition temperatures are summarized in the main text Table 1. Samples used for TGA were the same ones used for DSC analysis (see Figure S9), and were placed in 100 µl aluminum pans. The heating rate was 10 °C min^{-1}.The sample '0, uncrosslinked' was a liquid, and was dropped into the aluminum pan with a glass pipette.

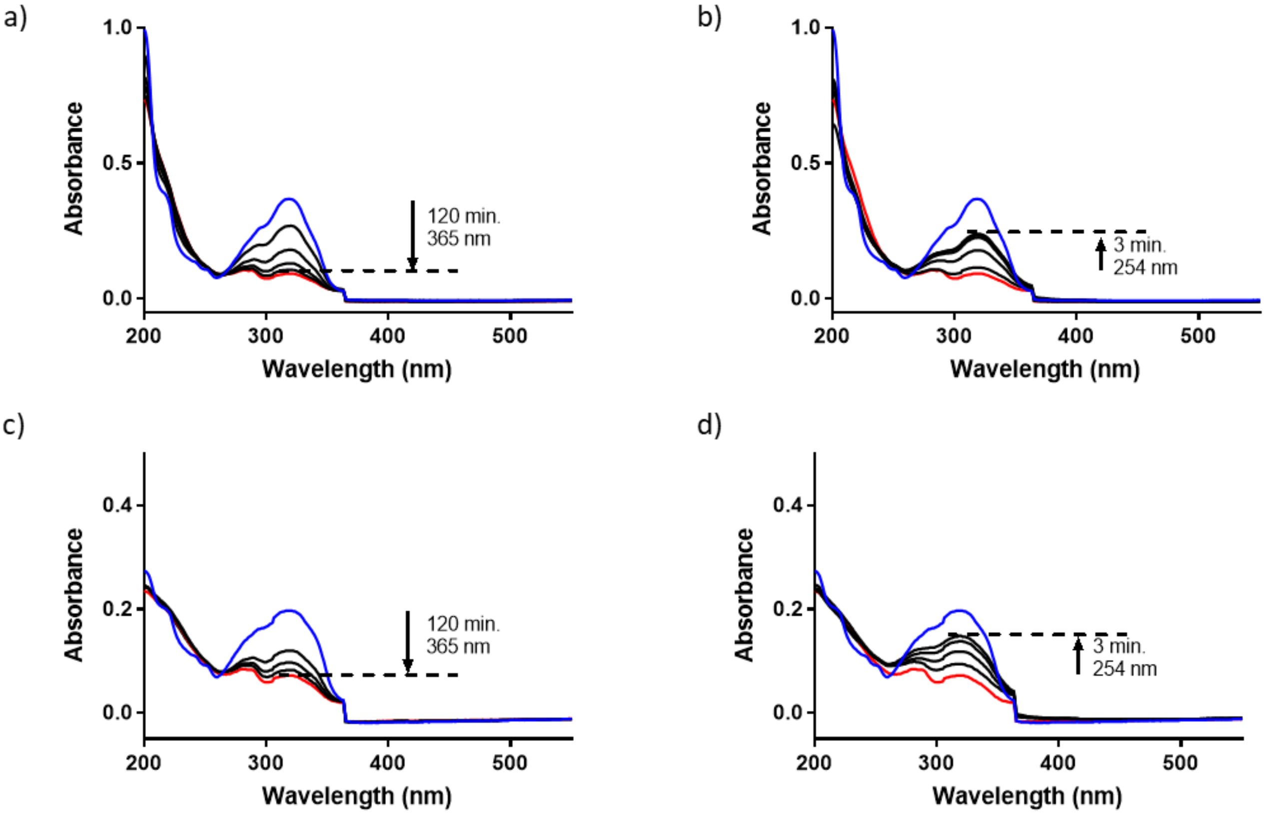

Figure S15. UV-Vis spectra of: APTS-GO/sPDMS 0.5/100 after crosslinking (a), and subsequent decrosslinking (b). sPDMS-24 after crosslinking (c), and subsequent decrosslinking (d). The blue lines indicate the film spectra without any UV exposure, and the red lines indicate the film spectra after reaching the maximum crosslinking amount *via* 120 min. 365 nm irradiation. The 325 nm peak corresponds to the enone's double bond, where a reduction by 365 nm indicates consumption of the double bond, and vice-versa. The formation of the cyclobutane ring can be traced by the peak around 285 nm, which follows an opposite trend with the 325 nm peak. Both samples were made by spin-coating a 12 wt.% solution in THF onto a square quartz substrate at 1500 rpm.

Table S4. Summary of the UV-Vis analysis on the sPDMS and APTS-GO/sPDMS 0.5/100.

Sample	Crosslinking conversion (%)[a]	Crosslinking conversion rate constant [K] (min^{-1})[b]	De-crosslinking conversion (%)[c]	De-crosslinking time needed for 50% conversion [K_d] (min) [d]
sPDMS	72	0.03139	75	0.06474
APTS-GO/sPDMS 0.5/100	82	0.02201	65	0.1295

[a] Conversion calculated from: % conversion = 1-($Absorbance_{120min}$/$Absorbance_{0\ min}$) *via* 365 nm irradiation, taking the 325 nm wavelength absorbance.

[b] Rate constant determined from exponential decay equation, [%enone = (%$enone_0$ - Plateau) * exp(-K*irradiation time) + Plateau)]

[c] Conversion calculated from: % conversion = ($Absorbance_{3min}$/$Absorbance_{0\ min}$) *via* 254 nm irradiation

[d] value determined from a hyperbola function, [%enone=$enone_{max}$ *irradiation time/(Kd+irradiation time)] *via* 254 nm irradiation, taking the 325 nm wavelength absorbance

Table S5. Summary of permeability, solubility, and diffusivity parameters of gases in PDMS at 35 °C. Taken with permission from Merkel *et al.*;[9] Copyright John Wiley & Sons, Inc.

Penetrant	Permeability (Barrer)[a]	Solubility (cm^3(STP) cm^{-3} atm^{-1})	Diffusivity *10^6 (cm^2 s^{-1})
H_2	890 ± 30	0.05 ± 0.008	140 ± 5
O_2	800 ± 20	0.18 ± 0.01	34 ± 1
N_2	400 ± 10	0.09 ± 0.008	34 ± 1
CO_2	3800 ± 70	1.29 ± 0.01	22 ± 1
C_3H_8	4100 ± 300	5.0 ± 0.07	5.1 ± 0.3

[a] 1 Barrer = 10^{-10} cm^3(STP) cm cm^{-2} s^{-1} cmHg^{-1}.

Figure S16. Left: spin-coating precursor solution. Right: AAO support coated with the APTS-GO/sPDMS layer. Both photos are for a 0.25 wt.% loading.

References

1. S. Honda and T. Toyota, *Polymer*, 2018, **148**, 211-216.
2. H. Yang, F. Li, C. Shan, D. Han, Q. Zhang, L. Niu and A. Ivaska, *J. Mater. Chem.*, 2009, **19**, 4632-4638.
3. P. Liu, Z. Yao, L. Li and J. Zhou, *Polym. Compos.*, 2016, **37**, 907-914.
4. J. Zhang, Q. Xin, X. Li, M. Yun, R. Xu, S. Wang, Y. Li, L. Lin, X. Ding, H. Ye and Y. Zhang, *J. Membr. Sci.*, 2019, **570-571**, 343-354.
5. S. Leaper, A. Abdel-Karim, B. Faki, J. M. Luque-Alled, M. Alberto, A. Vijayaraghavan, S. M. Holmes, G. Szekely, M. I. Badawy, N. Shokri and P. Gorgojo, *J. Membr. Sci.*, 2018, **554**, 309-323.
6. Z. Xu, J. Zhang, M. Shan, Y. Li, B. Li, J. Niu, B. Zhou and X. Qian, *J. Membr. Sci.*, 2014, **458**, 1-13.
7. D. G. Papageorgiou, Z. Li, M. Liu, I. A. Kinloch and R. J. Young, *Nanoscale*, 2020, **12**, 2228-2267.
8. T. Xu, C. Zhang, P. Li, X. Dai, L. Qu, Y. Sui, J. Gu and Y. Dou, *New J. Chem.*, 2018, **42**, 13873-13883.
9. T. C. Merkel, V. I. Bondar, K. Nagai, B. D. Freeman and I. Pinnau, *J. Polym. Sci., Part B: Polym. Phys.*, 2000, **38**, 415-434.